buildings

MDPI

Article

Modular Construction of Topological Interlocking Blocks—An Algebraic Approach for Resource-Efficient Carbon-Reinforced Concrete Structures

Sascha Stüttgen [1,*], Reymond Akpanya [2], Birgit Beckmann [3], Rostislav Chudoba [4], Daniel Robertz [1] and Alice C. Niemeyer [2]

[1] Chair of Algebra and Number Theory, RWTH Aachen University, 52062 Aachen, Germany; daniel.robertz@rwth-aachen.de
[2] Chair of Algebra and Representation Theory, RWTH Aachen University, 52062 Aachen, Germany; akpanya@art.rwth-aachen.de (R.A.); alice.niemeyer@art.rwth-aachen.de (A.C.N.)
[3] Institute of Concrete Structures, Technische Universität Dresden, 01069 Dresden, Germany; birgit.beckmann@tu-dresden.de
[4] Institue of Structural Concrete, RWTH Aachen University, 52062 Aachen, Germany; rostislav.chudoba@rwth-aachen.de
* Correspondence: sascha.stuettgen@rwth-aachen.de; Tel.: +49-(0)241-8094-534

Abstract: An algebraic approach to the design of resource-efficient carbon-reinforced concrete structures is presented. Interdisciplinary research in the fields of mathematics and algebra on the one hand and civil engineering and concrete structures on the other can lead to fruitful interactions and can contribute to the development of resource-efficient and sustainable concrete structures. Textile-reinforced concrete (TRC) using non-crimp fabric carbon reinforcement enables very thin and lightweight constructions and thus requires new construction strategies and new manufacturing methods. Algebraic methods applied to topological interlocking contribute to modular, reusable, and hence resource-efficient TRC structures. A modular approach to construct new interlocking blocks by combining different Platonic and Archimedean solids is presented. In particular, the design of blocks that can be decomposed into various n-prisms is the focus of this paper. It is demonstrated that the resulting blocks are highly versatile and offer numerous possibilities for the creation of interlocking assemblies, and a rigorous proof of the interlocking property is outlined.

Keywords: carbon-reinforced concrete; textile-reinforced concrete TRC; topological interlocking; Platonic solids; Archimedean solids; concrete structures; computational form finding

Citation: Stüttgen, S.; Akpanya, R.; Beckmann, B.; Chudoba, R.; Robertz, D.; Niemeyer, A.C. Modular Construction of Topological Interlocking Blocks—An Algebraic Approach for Resource-Efficient Carbon-Reinforced Concrete Structures. *Buildings* **2023**, *13*, 2565. https://doi.org/10.3390/buildings13102565

Academic Editors: Binsheng (Ben) Zhang and Ramadhansyah Putra Jaya

Received: 4 September 2023
Revised: 5 October 2023
Accepted: 6 October 2023
Published: 10 October 2023

1. Introduction

1.1. Carbon-Reinforced Concrete

Non-metallic reinforcement opens up a completely new field for concrete structures and therefore requires new construction strategies and new manufacturing methods [1]. One of the key properties of textile-reinforced concrete (TRC) or carbon-reinforced concrete (CRC) is the corrosion resistance of carbon, which leads to several benefits. The concrete cover needed for carbon reinforcement is much smaller than that needed for steel reinforcement. Hence, components can be very thin and lightweight, yielding a path to resource-efficient and sustainable construction. Currently, existing design principles of steel-reinforced concrete are being applied to carbon-reinforced concrete. While this is already yielding benefits and shows the applicability of carbon-reinforced concrete, it does not exploit its full potential. Applying those classical design principles to carbon-reinforced concrete and solely replacing the reinforcing steel with carbon results in load-bearing TRC structures that either exhibit large deformations or low material utilization, as quantitatively analyzed [2,3]: when carbon-reinforced concrete is used for classical components such as beams, exhausting the full load-bearing capacity will lead to deformations due

to low material thickness. On, the other hand, if serviceability requirements are met, e.g., deformations and deflections are small, the material will be subjected to small stresses and thus under-utilized, leading to a waste of resources (see ref. [2]). Hence, in order to exploit the full potential of carbon-reinforced concrete as a composite material and to design load-bearing structures that exhibit both low deformations and high material utilization, new material-appropriate design principles are required.

Since thin components show low bending stiffness compared to the capacity for normal forces, carbon-reinforced concrete is especially suited to the principles of lightweight constructions, in cases where out-of-plane bending is mostly avoided. The avoidance of bending makes sense, since bending means maximum stresses and strains in the outer regions of the cross section only. In the central regions of the cross section, the stresses and strains are small and the material is under-utilized. This means that most of a bending component is a waste of material and therefore resource-consuming. New design principles for carbon-reinforced concrete are required instead, where various approaches are pursued [4]. These include consideration of the reinforcement cross sections [2], in-plane bending of facets or sheets (since this can be highly efficient in contrast to out-of-plane bending), and external or internal shell structures [5–7]. From an ecological perspective, material-appropriate and resource-efficient construction is a very challenging task and important duty—especially when dealing with problems such as climate change and resource scarcity.

Another essential property of textile-reinforced concrete is that it can be folded while it is still fresh. This is not the case for steel-reinforced concrete. It is possible to create folds and folded structures that form large spans with low material input and high resource efficiency (see ref. [8]). To achieve folded structures and folding plans, triangulations are needed.

1.2. Algebra in Civil Engineering

What do civil engineering and algebra have to do with each other? Exploiting algebraic methods can give new insights into the study of construction methods that are already established in civil engineering. On the other hand, algebraic results often lead to unforeseen applications in engineering disciplines. An example of this observation is the triangulation of surfaces. Triangulations can be used to generate folding plans, as required for the production of folded structures. Folding is one of the key design strategies to combine both serviceability and material utilization. Furthermore, a folded structure comprises ductile behaviour, whereby the ductility is achieved at the structural instead of the material level. An example is the comparison of the ductility of a flat sheet and the same sheet folded in a waterbomb pattern. By varying the parameters of a waterbomb folding pattern, for example, the edge lengths and folding angles of the base cell, global shell shapes in a wide spectrum can be achieved [8–10], thereby changing its properties at a structural level (see Figure 1).

An example of a triangulation is the Delaunay triangulation. It is very common in civil engineering and in numerical simulations based on the finite element method (FEM). This decomposition of a surface into subsurfaces is the starting point for virtually any discretization of geometry in FE numerical simulations. From an algebraic point of view, however, this triangulation is only one possible triangulation. Thus, in addition to formulating the folding plans, algebraic methods of triangulation can also serve as inspiration for new carbon concrete structures. Triangulations of surfaces have been studied for some time in mathematics and computer science. Both the Delaunay triangulation, in which a triangulated surface is created using a given set of support points, and the Voronoi tessellation dual to this, in which a given surface is mosaiced into polygons based on support points, are commonly used in engineering. In addition to these two well-known methods, there are more general methods to create parameterized surfaces as well as to triangulate implicitly given surfaces. As a rule, the closest possible approximation to the given surface is obtained by a large number of very different and not necessarily planar triangles. An extensive body of literature deals with this subject, and as an example of a

review source, consider [11]. Instead of approximating a given surface by triangulation, other problems inspired from an architectural view can be targeted. Namely, it can be investigated which triangulated surfaces can be created from triangles with a specific congruence type. Research on the theory of particular surfaces controlled by one triangle is presented in refs. [12–14].

Figure 1. (**a**,**b**) Waterbomb folding structure: different choices of folding angles of the base cell lead to different curvature of the whole waterbomb structure; (**c**,**d**) Photograph of a carbon-reinforced concrete roof prototype folded using origami tessellation kinematics (Photographs: Rostislav Chudoba).

1.3. Interlocking

The principle that is examined algebraically in this paper to inspire new design principles for TRC structures is the notion of topological interlocking assemblies. It enables the design of structures consisting of building blocks that do not require any mortar in order to ensure structural stability. This is especially interesting in the context of sustainable, modular, recyclable, and reusable construction with concrete. Topological interlocking finds frequent application within compression-loaded structures, notably in contexts such as dry-stone walls and masonry, as exemplified in ref. [15]. In the late 17th century, Joseph Abeille unveiled his invention of the Abeille tile to the French Academy of Sciences [16] (see Figure 2). This innovative tile could be arranged in a manner that effectively immobilized each individual tile through its connection with adjacent tiles.

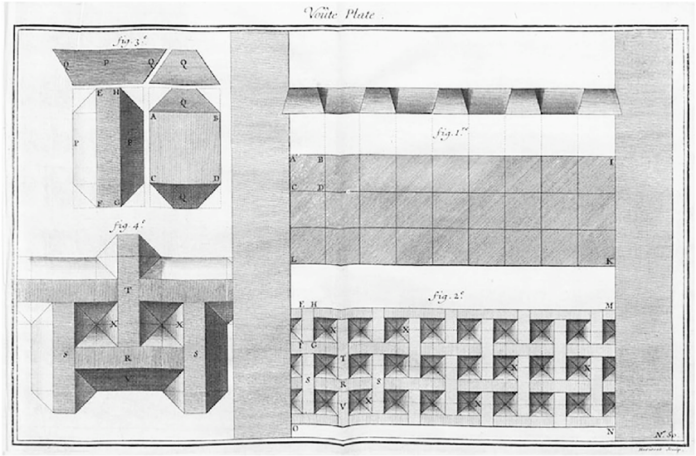

Figure 2. Joseph Abeille's proposed stone tile [16].

The idea of interlocking blocks has also been investigated by Glickmann [17]. In his search for a vertically interlocking pavement, he presented the G-Block. The design of this block is based on the tetrahedron and its corresponding tetrahedra interlocking to form an early example of an interlocking system. Since the work of Dyskin et al. (see ref. [18] and subsequent publications), topological interlocking has been the focus of extensive research. For a recent overview, refer to ref. [19].

1.3.1. Analogy and Explanation

When building an assembly of elements, e.g., a wall made of stones, the stones can be fixed using mortar. As a result, the elements (stones) cannot move out of the assembly. When elements or blocks are fixed amongst each other solely due to their geometric shape, they are said to be interlocked. In that case, a fixation is achieved without using mortar. On an engineering level, stereotomic architecture, i.e., the principle of interlocking, has been used for a long time and derived design principles can be seen in constructions such as stone arcs (see Figure 3). For the erection of such an arc, a temporary arch-shaped formwork or subconstruction, e.g., made of wood, is needed. The individual stones are placed on the subconstruction. They are not yet locked and can easily be removed. Only when the arch is entirely filled with stones do the stones jam each other so that no stone can fall, and the formwork subconstruction can be removed. Once the final stone—mostly the middle one—is placed into the arc, the flux of force through the jammed stones is established. Since the final stone functions as a key from a technical point of view, it is often decorated and emphasized. From an engineering point of view and under gravity, this example illustrates the principle of interlocking, even though such a construction is not a topological interlocking according to the formal mathematical definition, which is outlined in the next section.

Figure 3. A stone arc is stable only when all stones are included (Photograph: Franz Vincentz [20]).

1.3.2. Mathematical Description

Mathematically, a topological interlocking assembly is an assembly of rigid blocks together with a fixed frame, so that any subset of blocks is kinematically constrained and therefore cannot be removed from the assembly. The concept of topological interlocking as a material design concept was pioneered by Dyskin, Estrin, Kanel-Belov, and Pasternak [18,19]. For instance, the authors Dyskin et al. show that it is possible to form topological interlocking assemblies by assembling copies of one of the Platonic solids. The cube and the tetrahedra interlocking assemblies are illustrated in Figure 4.

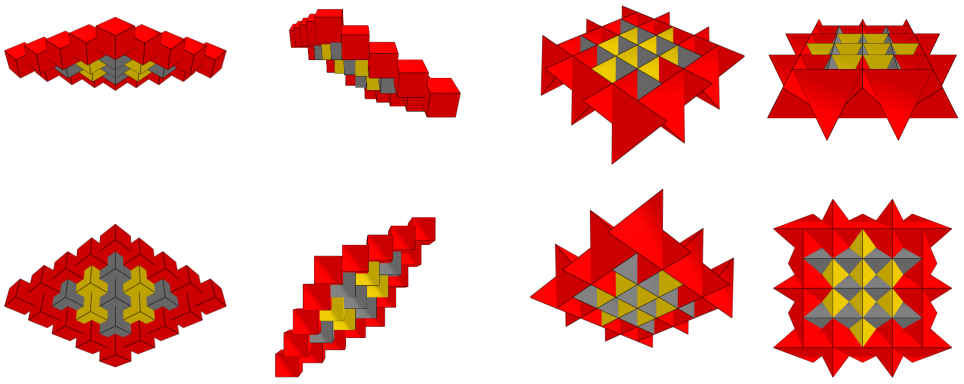

(**a**) (**b**)

Figure 4. (**a**) Cube interlocking; (**b**) Tetrahedra interlocking. The frame is shown in red.

A modular approach to designing new blocks that enable topological interlocking assemblies is the primary focus of this paper. In this paper, a focus is placed on new

topological interlocking blocks that can be disassembled into various Archimedean and Platonic solids. In particular, a demonstration of the modular approach used to design more complex geometries with interlocking properties by combining different regular prisms is presented. Furthermore, it is shown that these topological interlocking blocks exhibit versatility, as they can be arranged into various topological interlocking assemblies. To achieve this, a definition of topological interlocking, along with the concept of convex sets, is presented in Section 2, in order to provide a foundational understanding of the interlocking blocks constructed in this paper. In Section 3, the construction methods are introduced, and examples of topological interlocking blocks that can be deconstructed into different regular prisms are provided. More precisely, topological interlocking blocks that can be assembled from one regular n-prism and six regular 3-prisms in Section 3.2.1, or one regular n-prism and six cubes in Section 3.2.2, are introduced. Various possibilities for forming corresponding interlocking assemblies are discussed. Additionally, it is demonstrated that these assemblies indeed qualify as topological interlocking assemblies by building upon an interlocking test introduced in ref. [21] and generalizing it to certify the interlocking property for more kinds of interlocking assemblies, in particular the ones presented in this paper. Algorithms and functions to analyze the presented blocks and their topological interlocking assemblies are implemented in the programming language Julia [22] using the packages Polyhedra, v0.7.6, [23] for convex polyhedron computations and JuMP, v1.15.1, [24] for linear programming in combination with the Julia wrapper of the C solver HiGHS, v1.7.2, [25]. The images were generated using the Julia package PlotlyJS, v0.18.10, [26]. The source code has been made public under the second author's GitHub page [27]. Furthermore, the GAP package SimplicialSurfaces can be exploited to study the blocks' combinatorial properties [28,29].

1.3.3. Using Topological Interlocking in the Design of Carbon Concrete Components

Novel interlocking blocks that can be assembled in various configurations are provided through the presented constructions. This fact opens up new possibilities for modular CRC structures. The modularisation of structural members in construction is very important for resource efficiency, the extension of life cycles of different components and the reuse of units, especially in connection with new manufacturing processes. For reusability of components, interlocking principles can be a valuable approach. If an assembly is interlocked from many modules and fixed only by a spanning frame, no glue or material connections are required between the modules. If the fixing frame is omitted, the modules can easily be detached from each other. The avoidance of glue or any bonding agent between the blocks or elements is a key property for repeatable and wasteless decomposability. Thus, interlocking enhances the life cycle and sustainability of concrete structures.

In ongoing and unpublished research in the framework of the Collaborative Research Centre CRC/TRR 280 "Design Strategies for Material-Minimized Carbon Reinforced Concrete Structures Principles of a New Approach to Construction", a different type of interlocking block, distinct from the ones presented in this study, has been produced through concrete 3D printing and subjected to preliminary testing [30]. It is also the primary aim of the presented research to fabricate the described blocks using the CRC 3D printing methods currently in development [31,32], followed by comprehensive testing to assess their real-world applicability and iterative design refinement. The topological interlocking assemblies constructed in this paper serve as an inspiration for the construction of decomposable concrete columns and the transition of a column to a load-bearing ceiling construction.

2. Methods

In this section, the fundamental definitions and concepts required to introduce the construction of topological interlocking blocks and their respective assemblies in Section 3 are presented.

2.1. Convex Hull

As the objective of this paper is to create topological interlocking blocks by combining various prisms, it is essential to provide a description of these three-dimensional bodies that facilitates further examination of these structures. In this context, the notion of generating convex hulls from finite sets of 3D points as a means to achieve the intended construction of interlocking blocks is revisited.

Therefore, let $M = \{v_1, \ldots, v_n\} \subset \mathbb{R}^3$ be such a set of 3D points. The *convex hull* $\mathrm{conv}(M)$ of these points is defined by

$$\mathrm{conv}(M) := \left\{ \sum_{i=1}^{n} a_i v_i \mid \sum_{i=1}^{n} a_i = 1, a_i \geq 0 \right\}.$$

The set M is called the *vertex set* of $\mathrm{conv}(M)$. A set $F \subset \mathrm{conv}(M)$ is called a *facet* of $\mathrm{conv}(M)$ if it is the convex hull of a maximal coplanar set $P \subseteq M$, i.e., $F = \mathrm{conv}(P)$. Furthermore, a set $f \subset \mathrm{conv}(M)$ is called a *subfacet* of $\mathrm{conv}(M)$, if it is the convex hull of a coplanar but not colinear subset P of M.

Example 1. *For instance, a cube can be constructed by taking the convex hull of the following set (see Figure 5):*

$$\{(0,0,0)^t, (1,0,0)^t, (1,1,0)^t, (0,1,0)^t, (0,0,1)^t, (1,0,1)^t, (1,1,1)^t, (0,1,1)^t\}.$$

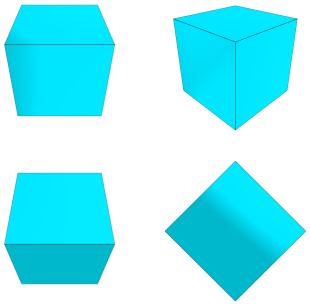

Figure 5. A cube.

The cube defined above has exactly 6 facets. For example, one of those facets is given by

$$F = \mathrm{conv}(\{(0,0,0)^t, (1,0,0)^t, (1,1,0)^t, (0,1,0)^t\}).$$

Moreover, the set $f = \mathrm{conv}(\{(0,0,0)^t, (1,0,0)^t, (0,1,0)^t\})$ *is an example of a subfacet of the above cube.*

With the notion of a convex hull, regular prisms, which are essential for the constructions of the topological interlocking blocks, can be defined. Let therefore $n \geq 3$ be a natural number. An *n-prism* is the three-dimensional body that arises from taking the convex hull of the set

$$M = \left\{ \left(\alpha \cdot \cos\left(\frac{2\pi k}{n}\right), \alpha \cdot \sin\left(\frac{2\pi k}{n}\right), h \right)^t \mid k = 0, \ldots, n-1, h = 0, 1 \right\},$$

where $\alpha = \left\| (\cos(0), \sin(0))^t - (\cos(2\pi/n), \sin(2\pi/n))^t \right\|^{-1}$.

Figure 6 illustrates the resulting three-dimensional body for $n = 6$ and $n = 8$.

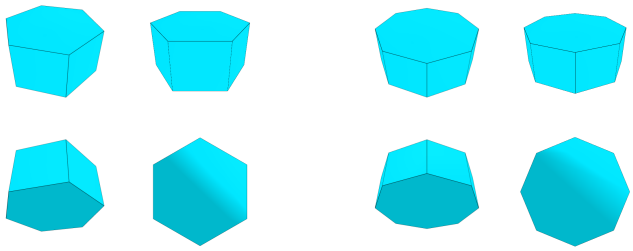

(**a**) (**b**)

Figure 6. (**a**) A regular 6-prism; (**b**) A regular 8-prism.

Note that for $n \neq 4$, an n-prism has exactly two types of facets, namely, two facets that form regular n-gons with edge lengths 1 and n facets forming squares with edge lengths 1. For $n = 4$, the resulting structure is the well-known cube with six squares as facets.

Remark 1. *It is also possible to model the prisms as polygonal complexes and manipulate the underlying incidence structure to obtain a more precise description of these structures and the merging of different prisms. Here, the decision is made to describe the different blocks by defining suitable convex sets to facilitate the construction of the topological interlocking blocks and their corresponding assemblies.*

2.2. Topological Interlocking

In this subsection, the concept of topological interlocking assemblies is introduced. More precisely, an abbreviated definition of a topological interlocking assembly, as found in ref. [33], is revisited. Furthermore, established procedures for computationally testing whether a given assembly meets the criteria of being a topological interlocking assembly are examined. Here, a topological interlocking assembly is defined as follows: Let $(X_i)_{i \in I}$ be a family of blocks, where a block X_i is a two-dimensional manifold with possible singularities and I is an index set. The family $(X_i)_{i \in I}$ is a topological interlocking assembly for a given frame of fixed blocks $J \subset I$ if the following holds:

1. $(X_i)_{i \in I}$ is an assembly, that is, any two blocks can only intersect at their boundaries;
2. Any finite subset of blocks indexed by $S \subset I \setminus J$ cannot be moved using continuous motions (interlocking property).

A mathematically precise definition of a topological interlocking assembly can be found in ref. [34], where the authors introduce the notion of a family of continuous motions to establish the interlocking property. Further examples of topological interlocking assemblies can be found in ref. [33], where the authors exploit the idea of deforming tiles of a tessellated three-dimensional structure to construct topological interlocking blocks. Thus, the resulting assembly realizes the surface of the underlying structure. The corresponding topological interlocking that is based on the surface of a cube is illustrated in Figure 7. Here, any two blocks of the assembly can form the frame of the given assembly.

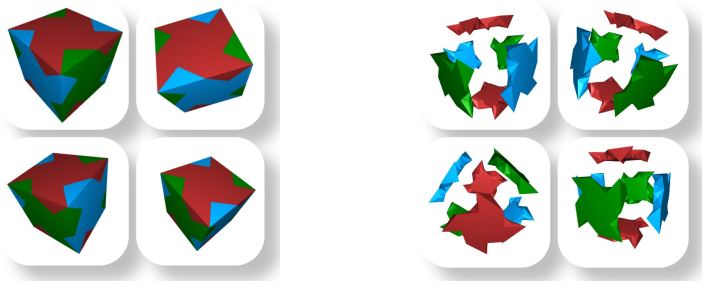

(**a**) (**b**)

Figure 7. (**a**) Assembled topological interlocking realizing the cube; (**b**) Exploded view of a topological interlocking assembly realizing the cube.

2.3. Infinitesimal Criterion for a Topological Interlocking

Showing that the interlocking property holds for a given assembly and therefore analyzing families of continuous motions that are applied to subsets of blocks of this assembly turn out to be tasks of high complexity. Thus, useful heuristics to support the task of verifying the interlocking property are essential. One such interlocking test can be found in ref. [21], where for a given assembly the authors present a linear optimization problem by introducing infinitesimal motions to the blocks of the assembly such that the interlocking property holds if the introduced optimization problem has no non-zero solutions. More details of the corresponding linear program are presented in Section 3.3.

3. Results

In this section, the blocks that are the focus of this paper are presented and analyzed. First, the different blocks designed by combining various regular prisms are introduced, and their corresponding assemblies are constructed. Furthermore, an investigation is conducted to determine whether the interlocking property is upheld for these assemblies. This assessment is carried out using the interlocking test proposed in ref. [21] and a modified version of this test.

3.1. Construction of the Blocks

Since the interest of this paper is designing more complex blocks by combining smaller convex bodies, a description of the merging of convex bodies is required. For simplicity, the *merging* of an n_1-prism and an n_2-prism is defined. Loosely speaking, the aim is to construct three-dimensional blocks by attaching the n_2-prism to the n_1-prism along a common face. More precisely, this is achieved by applying rigid transformations to the n_i-prisms. Let therefore S_1 and S_2 be an n_1- and n_2-prism, respectively. Furthermore, let F_i be a facet of S_i, respectively, with vertex sets $\{v_1, \dots, v_m\}$ and $\{w_1, \dots, w_m\}$. So, either $m = 4$ and the facets F_i are regular 4-gons or $n_1 = m = n_2$ and thus the facets F_i are regular m-gons. Without loss of generality, the vertex sets are indexed in such a way that

$$\|v_j - v_{j+1}\| = \|v_m - v_1\| = \|w_j - w_{j+1}\| = \|w_m - w_1\| = 1 \quad 1 \leq j \leq m-1,$$

where $\|x - y\|$ is the Euclidean distance between the points x and y. Since all vertices of a facet lie on a circle, it follows that $\|v_i - v_j\| = \|w_i - w_j\|$ for all $1 \leq i, j \leq m$. Thus, the following equality holds due to the law of cosines:

$$\measuredangle(v_2 - v_1, v_m - v_1) = \measuredangle(w_2 - w_1, w_m - w_1).$$

Here, the goal is to find a rigid transformation mapping w_i onto v_i and therefore achieving the alignment of the two prisms along the corresponding facets. More precisely, an affine map τ that preserves angles and distances, such that $\tau(w_j) = v_j$ for $1 \leq j \leq m$, is required. Since $w_2 - w_1$ and $w_m - w_1$ are linearly independent, there exists a unique matrix $A \in \mathbb{R}^{3\times3}$, such that

$$\begin{aligned} A(w_2 - w_1) &= v_2 - v_1, \\ A(w_m - w_1) &= v_m - v_1, \\ A((w_2 - w_1) \times (w_m - w_1)) &= -(v_2 - v_1) \times (v_m - v_1). \end{aligned}$$

Since A preserves the lengths and angles between basis vectors, it is an orthogonal matrix, and the map

$$\tau : \mathbb{R}^3 \to \mathbb{R}^3, \; x \mapsto A(x - w_1) + v_1$$

is an affine map with the desired properties. The *merging of* S_1 *and* S_2 *along the facets* F_1 *and* F_2 is then defined as the set $S_1 \cup \tau(S_2)$. Figure 8 shows all three-dimensional blocks that can be constructed by merging a 6-prism and an 8-prism along corresponding squares.

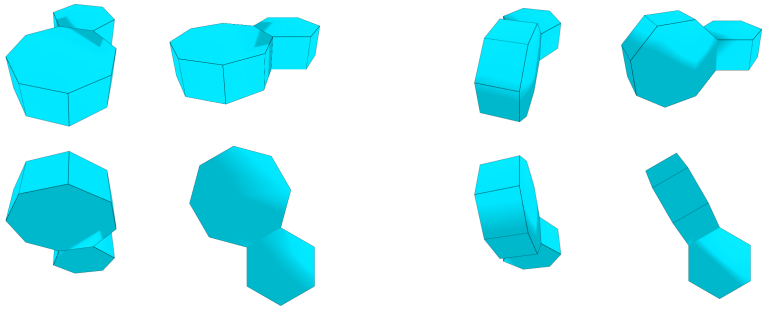

(**a**) (**b**)

Figure 8. Both possible mergings of an 8-prism and a 6-prism along a common square facet. (**a**) Merging without turning the blocks. (**b**) Merging after introducing a 90-degree rotation to the 6-prism.

3.2. Designing Topological Interlocking Blocks

In this section, different constructions leading to three-dimensional blocks that allow topological interlocking assemblies are presented and possible generalizations of those constructions are examined.

3.2.1. Designing Topological Interlocking Blocks by Attaching 3-Prisms

In this section, two constructions of topological interlocking blocks, which arise from merging copies of the 3-prism and an n-prism, and a discussion of their possible assemblies are presented.

Let therefore $n \geq 6$ be an even natural number, S be an n-prism, and F_1, F_2 be opposite square facets of S. A topological interlocking block is then constructed by applying the following procedure:

1. Merge three 3-prisms so that the resulting convex body is given by

$$\operatorname{conv}(\{(0,0,0)^t, (2,0,0)^t, \left(\frac{1}{2}, \frac{\sqrt{3}}{2}, 0\right)^t, \left(\frac{3}{2}, \frac{\sqrt{3}}{2}, 0\right)^t,$$
$$(0,0,1)^t, (2,0,1)^t, \left(\frac{1}{2}, \frac{\sqrt{3}}{2}, 1\right)^t, \left(\frac{3}{2}, \frac{\sqrt{3}}{2}, 1\right)^t\})$$

(see Figure 9b). This block shall be referred to as *3-hat*.

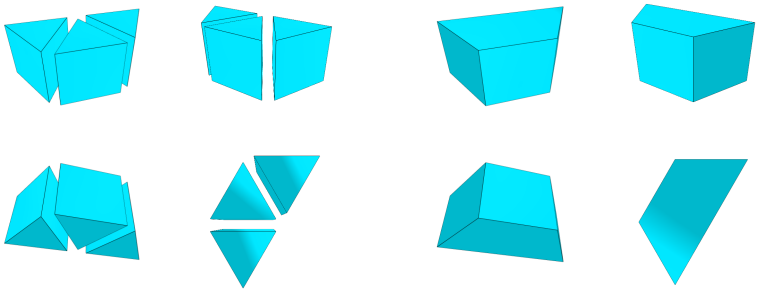

(**a**) (**b**)

Figure 9. (**a**) The 3-hat disassembled into three 3-prisms; (**b**) The merged 3-hat.

2. For $i = 1, 2$, merge S and a copy of the above block along the facet F_i and the facet of 3-hat given by

$$F = \operatorname{conv}\left(\left\{\left(\frac{1}{2}, \frac{\sqrt{3}}{2}, 0\right)^t, \left(\frac{3}{2}, \frac{\sqrt{3}}{2}, 0\right)^t, \left(\frac{1}{2}, \frac{\sqrt{3}}{2}, 1\right)^t, \left(\frac{3}{2}, \frac{\sqrt{3}}{2}, 1\right)^t\right\}\right).$$

such that no facet of the attached 3-hat is contained in the plane spanned by one of the regular n-gons that is a facet of S. The resulting block is called *n-candy*.

Figure 10 shows the blocks that arise from the above construction for $n = 6$ and $n = 8$ from different angles.

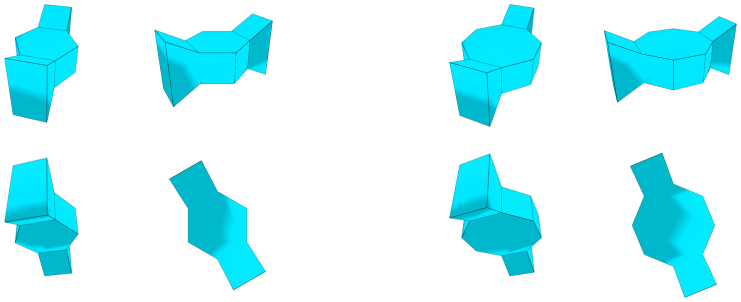

(**a**) (**b**)

Figure 10. n-candy for (**a**) $n = 6$; (**b**) $n = 8$.

These blocks are very versatile, since they allow different assemblies that are topologically interlocking. Here, three different assemblies of copies of the 6-candy and 8-candy that form topological interlocking assemblies are provided.

Application 1. The first assembly is constructed by stacking the blocks along the 6- and the 8-gon in a 2-periodic pattern introducing a 60-degree and 45-degree rotation every other block, respectively (see Figure 11). Fixing the top and bottom block as a frame for the assembly yields a topological interlocking in the sense of Section 2.2. The contacts between the central n-gons of the blocks restrict translational motion in the normal direction η of the contact surfaces and rotations not about η, while the 3-hats on the sides of the stacked n-gons constrain the translational motions parallel to the contact surfaces and rotations about η.

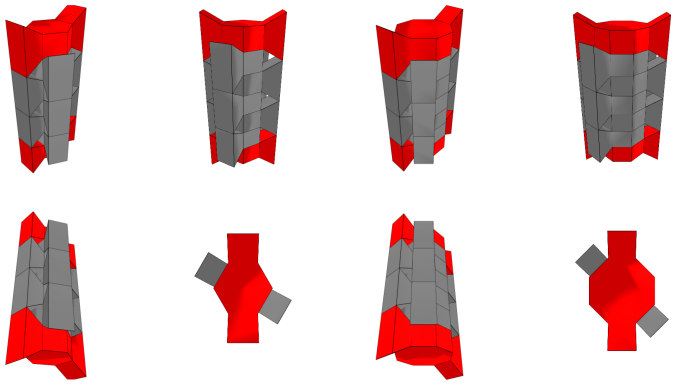

(**a**) (**b**)

Figure 11. The 2-periodic topological interlocking assemblies of the (**a**) 6-candy and (**b**) 8-candy. The frames are shown in red.

Application 2. The second assembly is achieved in a similar manner by stacking the blocks along the central n-gons. In this application, however, the assembly is constructed by a 3-periodic pattern. The second blocks in this pattern are obtained from the first one by introducing a 60-degree or 45-degree rotation about η and the third ones by rotating by

−60 or −45 degrees (see Figure 12). The same reasoning as above shows that this yields a topological interlocking assembly.

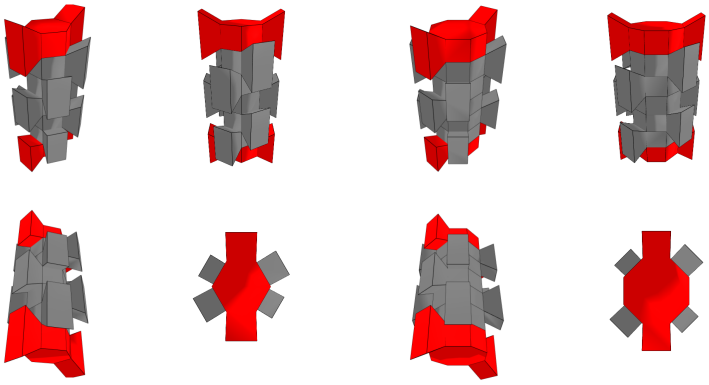

(**a**) (**b**)

Figure 12. The 3-periodic interlocking assemblies of the (**a**) 6-candy and (**b**) 8-candy. The frames are shown in red.

Application 3. The above assembly allows a wide range of arrangements of the introduced block, where the corresponding blocks of the assembly are not limited to being assembled in a stack. An example of such an assembly is illustrated in Figure 13. Pillars of the form described in Example 2 are taken, and they are connected by inserting another copy of the underlying block between two subassemblies.

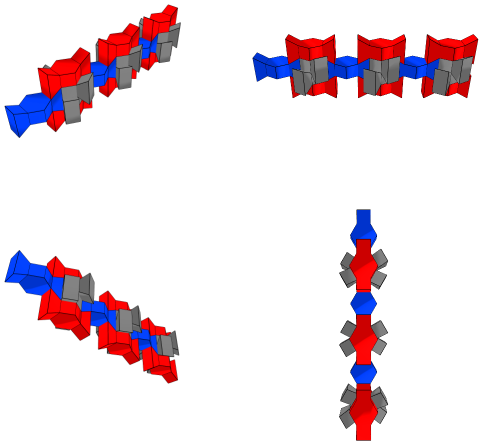

Figure 13. Interlocking assembly of the 6-candy as a linkage of the assemblies in Application 2 by inserting 6-candies between two pillars (blue). The frame is shown in red.

It is already known that the assemblies described in Application 2 interlock. Hence, by a symmetry argument it is enough to show that the subassembly shown in Figure 14 is topologically interlocking.

The subassembly itself contains a pillar as in Application 2 as a subassembly, so it is only necessary to show that the introduced block, indicated in blue, is kinematically constrained by the other blocks. This is easy to see as the frame constrains the new block in a way that only allows for it to slide out along a linear path perpendicular to the trapezoid faces of the attached 3-hats. This motion is restricted in both directions by the 3-hats attached to the two other blocks in contact with the new block. Thus, the block is kinematically constrained and the assembly in Figure 13 is topologically interlocked.

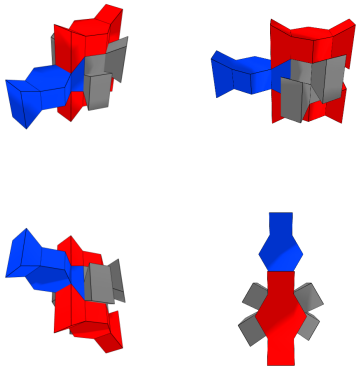

Figure 14. Subassembly of the assembly in Figure 13. The frame is coloured in red.

This construction can be generalized such that copies of the hat are attached to a subset of facets of S that form squares. For example, copies of the hat can be attached to every second square facet of S. This construction is illustrated in Figure 15 by attaching three 3-hats to the 6- and four to the 8-prism.

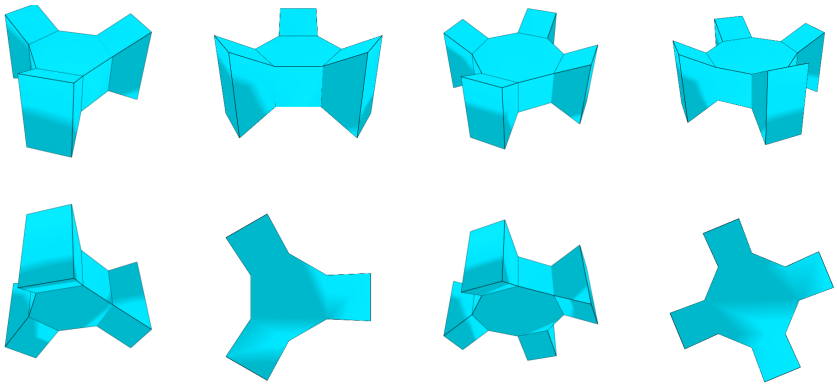

(**a**) (**b**)

Figure 15. Generalized (**a**) 6-candy and (**b**) 8-candy, where 3-hats are attached every second square facet.

Since more 3-hats are used in the generalized construction, the resulting blocks are not versatile and allow only one type of assembly. This type results from stacking copies of the block as seen in Figure 16. It is easy to see that this assembly of blocks indeed interlocks topologically; the assemblies in Applications 1 and 2 are a subset of the assembly below and thus they are topologically interlocking—attaching more copies of the 3-hat only adds further constraints to the motion of a block in the assembly.

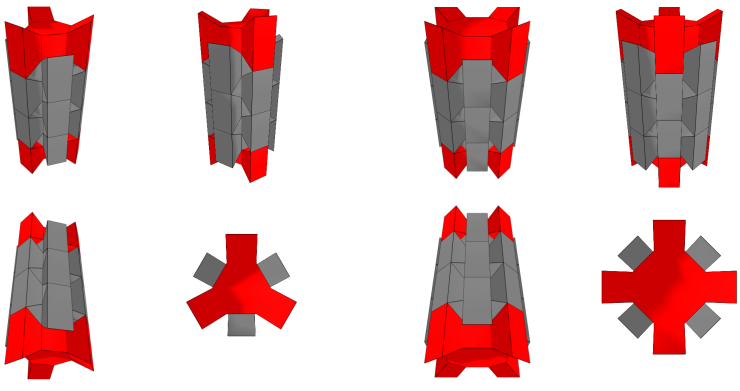

(**a**) (**b**)

Figure 16. The 2-periodic interlocking assemblies of the generalized (**a**) 6-candy and (**b**) 8-candy of Figure 15. The frames are shown in red.

3.2.2. Designing Topological Interlocking Blocks by Attaching Cubes

Inspired by the construction in Section 3.2.1, two constructions that yield topological interlocking blocks that can be decomposed into six copies of a cube (4-prism) and an n-prism are introduced. Moreover, possible topological interlocking assemblies are presented.

As in the above construction, let $n \geq 6$ be an even natural number, S be an n-prism, and F_1, F_2 be opposite square facets of S. Then, the *n-cube-candy* is defined by applying the following procedure:

1. Merge three cubes so that the resulting convex body is a cuboid with edge lengths 3 and 1. Such a convex body can be constructed by the following convex hull:

$$\begin{aligned}\operatorname{conv}(\{&(0,0,0)^t, (1,0,0)^t, (1,1,0)^t, (1,1,0)^t,\\ &(0,0,3)^t, (1,0,3)^t, (1,1,3)^t, (1,1,3)^t\}).\end{aligned}$$

   This block shall be referred to as *4-hat*.
2. As seen above, the n-prism S can be merged with a copy of the above block for $i = 1, 2$ along the facet F_i and the subfacet of 4-hat given by

$$F = \operatorname{conv}(\{(0,0,1)^t, (0,0,2)^t, (1,0,1)^t, (1,0,2)^t\})$$

   such that no facet of the 4-hat is contained in a plane spanned by one of the regular n-gons that is a facet of S.

For $n = 6$ and $n = 8$, the resulting n-cube-candies and a corresponding topological interlocking assembly analogous to the construction in Application 2 can be seen in Figures 17 and 18.

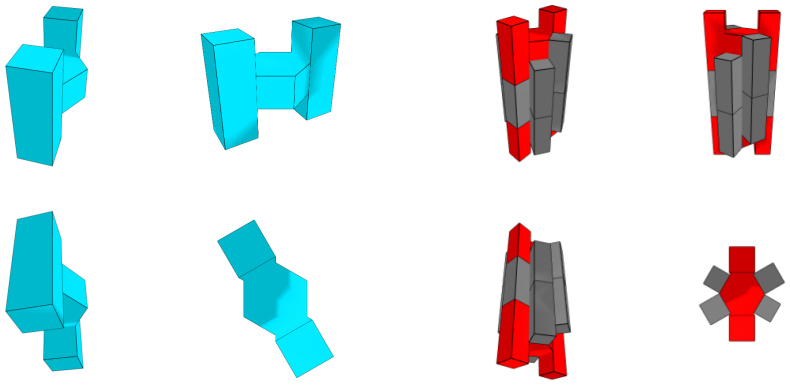

(**a**) (**b**)

Figure 17. (**a**) The 6-cube-candy and (**b**) its corresponding topological interlocking assembly analogous to the construction in Application 2. The frame is coloured in red.

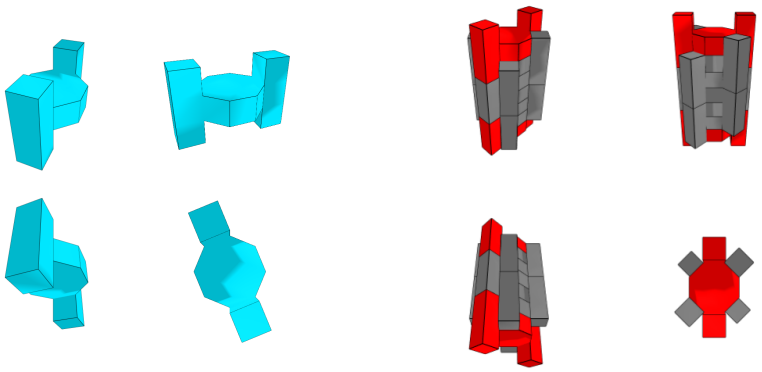

(**a**) (**b**)

Figure 18. (**a**) The 8-cube-candy and its (**b**) corresponding topological interlocking assembly analogous to the construction in Application 2. The frame is coloured in red.

Similar to the construction above, generalized versions of the constructed topological interlocking blocks by attaching copies of the 4-hat to a subset of the square facets of S (see Figure 15) are provided. In Figure 19, $n = 12$ and four 4-hats are attached to the 12-prism. The assembly is realized in a spiral pattern, where the blocks are stacked by introducing a 30-degree rotation at every step.

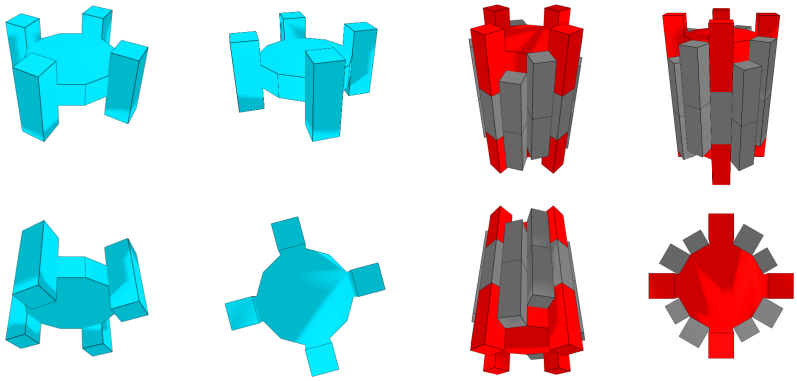

(**a**) (**b**)

Figure 19. (**a**) The 12-cube-candy and (**b**) a corresponding topological interlocking assembly following a spiral pattern. The frame is coloured in red.

Since the n-candy described in Section 3.2.1 is a subset of the n-cube-candy investigated in this subsection, the interlocking property of the assembly of the n-cube-candy can be established as in Section 3.2.1.

3.3. Proving the Interlocking Property

Next, some details for the rigorous verification of the interlocking property for the assemblies presented above are provided. This is achieved by building upon the existing interlocking test introduced by Wang et al. [21] and generalizing it.

Here, a brief summary of the details of the existing interlocking test is provided in order to emphasize the modifications that are implemented to derive an interlocking test capable of verifying the interlocking property for the topological interlocking blocks presented in this paper. For a more comprehensive description of the original interlocking test, the reader is directed to the publication by Wang et al.

Given an assembly of convex blocks, the algorithm proposed in ref. [21] produces a linear program whose solubility directly translates into a certificate of the interlocking property of the input assembly. For such an assembly, Wang et al. consider two types of contacts:

1. Contact points, i.e., zero-dimensional intersections, that result from the intersection of two non-parallel edges of two different blocks;
2. Contact facets (given as the convex set of a finite number of contact points), i.e., two-dimensional intersections, that result from the intersection of two facets of two different blocks.

These contact points form the foundation of the linear program. By introducing infinitesimal motions to the blocks (that can be expressed as a six-dimensional vector where the first three components correspond to the translation of the block and the last three components to its rotation), the computed contact points move according to the motions of the corresponding blocks. Wang et al. formulate linear constraints for the blocks not to intersect by requiring that the infinitesimal motion of the contact points relative to one of the blocks be restricted to the outside of that block. That is achieved by enforcing the relative infinitesimal motion of the contact points to be towards the halfspace not containing the reference block. Such a constraint is called *point–plane constraint* as it can be modelled as a point being restricted to one side of a plane. In particular, the authors model the different contacts in the following way:

1. For a contact point of two non-parallel edges, the necessary plane for the constraint is spanned by the corresponding two edges;
2. For each contact point of a contact facet, a constraint is derived by considering the plane spanned by the corresponding contact facet.

Thus, the indeterminates of the resulting linear program are the infinitesimal motions given by the translations and rotations of the different blocks. After adding the constraint for the frame blocks not to move, the interlocking property for a given assembly holds if the described linear program has no solutions besides the trivial zero solution.

Note that the convexity of the blocks is not required to formulate the above linear program. All that is needed is to be able to define an interior and an exterior of a given block, which is the case for the blocks described in this section. For the assemblies of the n-cube-candies illustrated in Figures 18 and 19, the formulation of the linear program described above already verifies the interlocking property of the given assemblies. On the other hand, for any of the assemblies of the n-candy presented in Section 3.2.1, the constraints considered by the linear program are not sufficient to prove the interlocking property as it finds non-zero solutions; since there are no edge–edge contacts of non-parallel edges, the constraints of the corresponding linear program only consist of the point–plane constraints arising from the two-dimensional intersection of facets of different blocks, i.e., the modelled contacts are solely the contacts of the n-prisms and thus the modelled assembly is equivalent to a pillar of stacked n-prisms. Intuitively, these contacts are not sufficient to establish the interlocking property in that case. The above test is therefore generalized by also modelling one-dimensional contacts between faces of different blocks, which will be called *contact edges*. There are three types of contact edges that can arise from an intersection of a block a with a block b:

1. An edge of block a intersects with a facet of block b. In that case, the point–plane constraints of the plane spanned by that facet for the corner points of the intersecting line segment is added. An example of such a contact is depicted in Figure 20. There, two cubes intersect at an edge of one cube and the interior of a facet of the other.

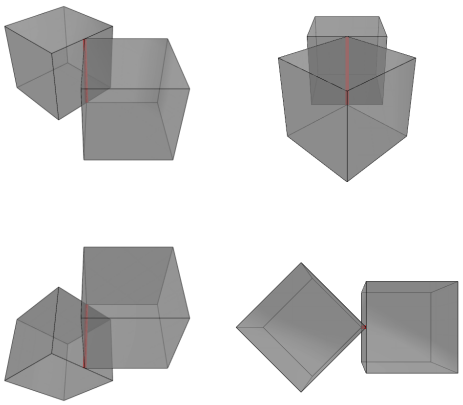

Figure 20. Two blocks with one-dimensional intersection between a facet and an edge. The contact between the blocks is coloured in red.

2. A convex edge of block a intersects a convex edge of block b. There are two facets of block a adjacent to the edge of a. In that case, it suffices that one of the two point–plane constraints of the planes spanned by those facets is fulfilled for both corner points of the intersecting line segment. This can be achieved by introducing a binary variable to the linear program that keeps track of which of the two constraints is fulfilled. An example of that contact type is the contact of two cubes along an edge. Figure 21 shows a picture of such a contact.

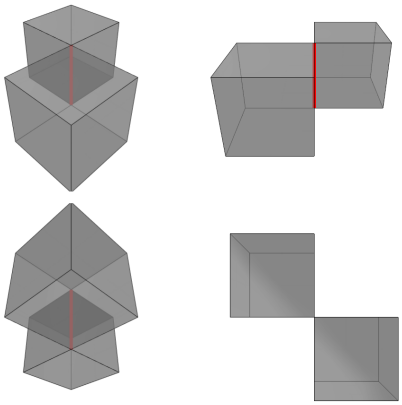

Figure 21. Two blocks with one-dimensional intersection between two convex edges. The contact between the blocks is coloured in red.

3. A concave edge of block a intersects a convex edge of block b. In that case, the feasible region for the infinitesimal motions of the contact points on b relative to a is convex. This is realized in the linear program by adding the point–plane constraints for both planes spanned by the facets of a adjacent to the concave edge for the corner points of the intersecting line segment. This contact type arises, for example, in the assembly in Application 1 (see Figure 22). Not modelling those contacts in the linear program is the reason why it is not possible to give a certificate of the interlocking property for the assemblies in Section 3.2.1 by applying the method proposed by Wang et al.

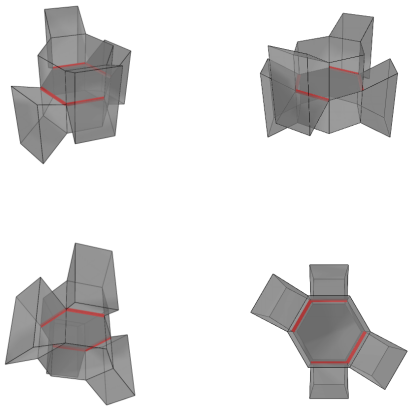

Figure 22. Two blocks with one-dimensional intersections between a convex and a concave edge. See Application 1. The one-dimensional contacts between the blocks are coloured in red.

Introducing this slight modification in the algorithm yields a linear program that verifies the interlocking property for the remaining assemblies in Section 3.2.1. Hence, the interlocking property holds for all the assemblies presented in Section 3.

4. Conclusions

The concept of topological interlocking harbours significant potential for enhancing the sustainability of concrete constructions, provided that the constituent blocks of an assembly can be manufactured efficiently. The proposed blocks are easily describable and offer versatility, as a single block type can be used to create various interlocking structures, promoting the reusability of building blocks. Since the presented modular approach to constructing interlocking blocks using different n-prisms can be extended to create interlocking blocks by combining arbitrary basic blocks, it facilitates the design of specialized construction kits for specific applications. In order to establish the interlocking property of the presented assemblies, an existing interlocking test [21] is extended to consider more general cases.

As described above, the focus of this paper is on blocks that can be decomposed into different n-prisms. Therefore, it might also be interesting to see more general constructions of blocks with interlocking properties. In a forthcoming publication, the second author will investigate the construction of topological interlocking blocks that can be decomposed into a finite number of octahedra and tetrahedra. Furthermore, the first and second authors will present the precise mathematical details of the implemented interlocking test in a future publication and will work on a Julia package based on the implementations in [27] to enable a user to manipulate and explore the combinatorial and geometrical properties of three-dimensional non-convex polyhedra.

Though the notion of topologically interlocking assemblies as a structural design concept has already been applied to build different structures, such as dry-stone and masonry walls, the applicability of the presented blocks still has to be tested. These tests include checking whether these blocks can be manufactured with concrete 3D printing [31], as well as numerical simulations and real-world tests of the interlocking property and failure behaviour of the concrete blocks under certain loads. It is acknowledged that realizing the blocks with 3D printing, as presented in this paper, appears to be quite challenging. Therefore, these blocks will undergo several design iterations to facilitate manufacturing with CRC 3D printing.

Author Contributions: Investigation: S.S., R.A. and B.B.; Software: S.S. and R.A.; Supervision, R.C., D.R. and A.C.N.; Visualization: S.S. and R.A.; Writing—original draft: S.S., R.A. and B.B.; Writing—review and editing: R.C., D.R. and A.C.N. All authors have read and agreed to the published version of the manuscript.

Funding: The authors gratefully acknowledge the funding by the Deutsche Forschungsgemeinschaft (DFG, German Research Foundation) in the framework of the Collaborative Research Centre CRC/TRR 280 "Design Strategies for Material-Minimized Carbon Reinforced Concrete Structures—Principles of a New Approach to Construction" (project ID 417002380).

Data Availability Statement: No new data were created or analyzed in this study. Data sharing is not applicable to this article

Conflicts of Interest: The authors declare no conflict of interest. The funders had no role in the design of the study; in the collection, analyses, or interpretation of data; in the writing of the manuscript; or in the decision to publish the results.

References

1. Beckmann, B.; Bielak, J.; Bosbach, S.; Scheerer, S.; Schmidt, C.; Hegger, J.; Curbach, M. Collaborative research on carbon reinforced concrete structures in the CRC/TRR 280 project. *Civ. Eng. Des.* **2021**, *3*, 99–109. [CrossRef]
2. Spartali, H.; Hegger, J.; Chudoba, R. Phenomenological comparison between the flexural performance of steel- and CFRP-reinforced concrete elements. *Eng. Struct.* **2023**, *294*, 116755. [CrossRef]
3. Preinstorfer, P.; Huber, T.; Reichenbach, S.; Lees, J.M.; Kromoser, B. Parametric Design Studies of Mass-Related Global Warming Potential and Construction Costs of FRP-Reinforced Concrete Infrastructure. *Polymers* **2022**, *14*, 2383. [CrossRef] [PubMed]
4. Beckmann, B.; Adam, V.; Marx, S.; Chudoba, R.; Hegger, J.; Curbach, M. Novel Design Strategies for Material-Minimized Carbon Reinforced Concrete Structures—Overview of the Research in CRC/TRR 280. In *Proceedings of the Building for the Future: Durable, Sustainable, Resilient*; Ilki, A., Çavunt, D., Çavunt, Y.S., Eds.; Springer: Cham, Switzerland, 2023; pp. 1242–1251.
5. Hawkins, W.; Orr, J.; Ibell, T.; Shepherd, P. A design methodology to reduce the embodied carbon of concrete buildings using thin-shell floors. *Eng. Struct.* **2020**, *207*, 110195. [CrossRef]
6. Vakaliuk, I.; Goertzen, T.; Scheerer, S.; Niemeyer, A.C.; Curbach, M. Initial Numerical Development of Design Procedures for TRC Bioinspired Shells. In Proceedings of the Innovation, Sustainability and Legacy—Proceedings of IASS/APCS 2022, Beijing, China, 19–22 September 2022; Xue, S.D., Wu, J.Z., Sun, G.J., Eds.; IASS International Association for Shell and Spatial Structures: Madrid, Spain, 2022; pp. 2597–2608.
7. Vakaliuk, I.; Scheerer, S.; Curbach, M. Initial Laboratory Test of Load-Bearing Shell-Shaped TRC Structures. In Proceedings of the Concrete Innovation for Sustainability—Proceedings for the 6th fib International Congress 2022, Oslo, Norway, 12–16 June 2022; Stokkeland, S., Braarud, H.C., Eds.; fib—International Federation for Structural Concrete: Lausanne, Switzerland, 2022; pp. 675–684.
8. Chudoba, R.; Brakhage, K. Rigid-Facet Kinematics Coupled with Finite Bending Rotation Along Crease Lines. In Proceedings of the 7th International Meeting on Origami in Science, Mathematics, and Education, Oxford, UK, 5–7 September 2018.
9. Chudoba, R.; Sharei, E.; Senckpiel, T.; Schladitz, F. Numerical Modeling of Non-Uniformly Reinforced Carbon Concrete Lightweight Ceiling Elements. *Appl. Sci.* **2019**, *9*, 2438. [CrossRef]

10. Chudoba, R.; van der Woerd, J.; Schmerl, M.; Hegger, J. ORICRETE: Modeling support for design and manufacturing of folded concrete structures. *Adv. Eng. Softw.* **2014**, *72*, 119–127. [CrossRef]
11. Bobenko, A.I.; Suris, Y.B. *Discrete Differential Geometry: Integrable Structure*; American Mathematical Society: Washington, DC, USA, 2008.
12. Brakhage, K.H.; Niemeyer, A.; Plesken, W.; Strzelczyk, A. Simplicial Surfaces Controlled by One Triangle. *J. Geom. Graph.* **2017**, *21*, 141–152.
13. Brakhage, K.H.; Niemeyer, A.C.; Plesken, W.; Robertz, D.; Strzelczyk, A. The icosahedra of edge length 1. *J. Algebra* **2020**, *545*, 4–26. [CrossRef]
14. Sulanke, T.; Lutz, F.H. Isomorphism-free lexicographic enumeration of triangulated surfaces and 3-manifolds. *Eur. J. Comb.* **2009**, *30*, 1965–1979. [CrossRef]
15. Moreno Gata, K.; Mueller, C.; Valiente, E. Designing Strategies for Topological Interlocking Assemblies in Architecture. Flat Vaults. In *Proceedings of the IASS Annual Symposium 2019, Structural Membranes 2019, Form and Force*; IASS International Association for shell and spatial structures: Madrid, Spain, 2019; ISSN 2518-6582.
16. Abeille, J. *Mémoire Concernant la Voûte Plate Inventée par M. Abeille*; Académie Royale des Sciences, Machines et Inventions Approuvées par l'Académie Royale des Sciences depuis son Établissement jusqu'à Present; avec Leur Description. Dessinées & Publiées du Consentement de l'Académie; Académie des Sciences: Paris, France, 1735; Volume 1, pp. 159–162. [CrossRef]
17. Glickmann, M. The G-Block System of Vertically Interlocking Paving. In Proceedings of the Second International Conference on Concrete Block Paving, Delft, The Netherlands, 10–12 April 1984.
18. Dyskin, A.; Estrin, Y.; Kanel-Belov, A.; Pasternak, E. A new concept in design of materials and structures: Assemblies of interlocked tetrahedron-shaped elements. *Scipta Mater.* **2001**, *44*, 2689–2694. [CrossRef]
19. Estrin, Y.; Krishnamurthy, V.R.; Akleman, E. Design of architectured materials based on topological and geometrical interlocking. *J. Mater. Res. Technol.* **2021**, *15*, 1165–1178. [CrossRef]
20. Vincentz, F. Schlussstein von 1788 in einem Torbogen des Wymeerer Glockenturms. Available online: https://commons.m.wikimedia.org/wiki/File:Bunde_Wymeer_-_Kirchstra%C3%9Fe_-_Glockenturm_07_ies.jpg (accessed on 3 September 2023).
21. Wang, Z.; Song, P.; Isvoranu, F.; Pauly, M. Design and Structural Optimization of Topological Interlocking Assemblies. *ACM Trans. Graph.* **2019**, *38*, 193. [CrossRef]
22. Bezanson, J.; Edelman, A.; Karpinski, S.; Shah, V.B. Julia: A fresh approach to numerical computing. *SIAM Rev.* **2017**, *59*, 65–98. [CrossRef]
23. Legat, B. Polyhedral Computation, JuliaCon 2023, Cambridge, MA, USA. 2023. Available online: https://pretalx.com/juliacon2023/talk/JP3SPX/ (accessed on 3 September 2023).
24. Lubin, M.; Dowson, O.; Dias Garcia, J.; Huchette, J.; Legat, B.; Vielma, J.P. JuMP 1.0: Recent improvements to a modeling language for mathematical optimization. *Math. Program. Comput.* **2023**. [CrossRef]
25. Huangfu, Q.; Hall, J.A.J. Parallelizing the dual revised simplex method. *Math. Program. Comput.* **2018**, *10*, 119–142. [CrossRef]
26. Plotly Technologies Inc. *Collaborative Data Science*; Plotly Technologies Inc.: Montreal, QC, Canada, 2015. Available online: https://plot.ly (accessed on 3 September 2023).
27. Akpanya, R.; Stüttgen, S. *Non-Convex-Interlocking*, Version 0.1; GitHub: San Francisco, CA, USA, 2023. Available online: https://github.com/ReymondAkpanya/Non-convex-Interlocking- (accessed on 3 September 2023).
28. Akpanya, R.; Baumeister, M.; Görtzen, T.; Niemeyer, A.; Weiß, M. *SimplicialSurfaces—A GAP Package*, Version 0.6. 2023. Available online: https://github.com/gap-packages/SimplicialSurfaces (accessed on 3 September 2023).
29. The GAP Group. GAP—Groups, Algorithms & Programming, Version 4.12.2. 2022. Available online: https://www.gap-system.org (accessed on 3 September 2023).
30. Neef, T. Schalenstrukturen aus Verriegelungsblöcken. 2023. Available online: https://www.sfbtrr280.de/news/news/detail/schalenstrukturen-aus-verriegelungsbloecken (accessed on 5 October 2023).
31. Neef, T.; Dittel, G.; Scheurer, M.; Gries, T.; Mechtcherine, V. Utilizing Textiles as Integrated Formwork for Additive Manufacturing with Concrete. In *Proceedings of the Building for the Future: Durable, Sustainable, Resilient*; Ilki, A., Çavunt, D., Çavunt, Y.S., Eds.; Springer: Cham, Switzerland, 2023; pp. 1285–1292. [CrossRef]
32. Neef, T.; Müller, S.; Mechtcherine, V. Integration of Mineral Impregnated Carbon Fibre (MCF) into Fine 3D-Printed Concrete Filaments. In *Proceedings of the Third RILEM International Conference on Concrete and Digital Fabrication*; Buswell, R., Blanco, A., Cavalaro, S., Kinnell, P., Eds.; Springer: Cham, Switzerland, 2022; pp. 397–403. [CrossRef]
33. Akpanya, R.; Goertzen, T.; Niemeyer, A. A Group-Theoretic Approach for Constructing Spherical-Interlocking Assemblies. In Proceedings of the Annual Symposium of the International Association for Shell and Spatial Structures (IASS 2023), Melbourne, Australia, 10–14 July 2023.
34. Goertzen, T.; Niemeyer, A.; Plesken, W. Topological Interlocking via Symmetry. In Proceedings of the 6th FIB International Congress 2022, Oslo, Norway, 12–16 June 2022; Novus Press: Oslo, Norway, 2022.